# Full counting statistics in the many-body Hatano-Nelson model

Balázs Dóra[1,2,*] and Cătălin Paşcu Moca[3,4]

[1]*MTA-BME Lendület Topology and Correlation Research Group, Budapest University of Technology and Economics, 1521 Budapest, Hungary*

[2]*Department of Theoretical Physics, Budapest University of Technology and Economics, 1521 Budapest, Hungary*

[3]*MTA-BME Quantum Dynamics and Correlations Research Group, Institute of Physics, Budapest University of Technology and Economics, 1521 Budapest, Hungary*

[4]*Department of Physics, University of Oradea, 410087 Oradea, Romania*

(Received 5 September 2022; accepted 29 November 2022; published 14 December 2022)

We study non-Hermitian many-body physics in the interacting Hatano-Nelson model with an open boundary condition. The violation of reciprocity, resulting from an imaginary vector potential, induces the non-Hermitian skin effect and causes exponential localization for all single-particle eigenfunctions in the noninteracting limit. Nevertheless, the density profile of the interacting system becomes only slightly tilted relative to the average filling. The Friedel oscillations exhibit a beating pattern due to the modification of the Fermi wave number. The probability distribution of particles over any finite interval is the normal distribution, whose mean scales with the imaginary vector potential and the variance is symmetric to the center of the chain. This is confirmed by several numerically exact methods even for relatively small systems. These features are expected to be generic not only for fermions, which naturally repel each other due to Pauli's exclusion principle, but for interacting bosons as well. Our findings indicate that many-body effects can significantly alter and conceal the single-particle properties and the skin effect in non-Hermitian systems.

DOI: 10.1103/PhysRevB.106.235125

## I. INTRODUCTION

In the theory of probability, a classical random variable is often successfully characterized by a few of its first moments, and the powerful laws that follow, such as the central limit theorem [1], have found numerous applications in diverse areas of science [2]. In many cases, however, this approach ceases to be satisfactory, and the full probability distribution function is needed as it reveals salient features about the random variable [3]. The quantum world is not much different in this respect from the classical one. Already simple expectation values of physical quantities often display rather complex behavior, and their complete understanding requires a lifelong effort, such as, e.g., the phase diagram of the Hubbard model [4]. Although they are often difficult to access, higher moments of the observables encapsulate unique information about nonlocal, multipoint correlators and entanglement and contain much more information. Finding all these moments is essentially equivalent to determining the entire distribution function of the quantity of interest, i.e., the characteristic function of full counting statistics [5–11].

Recent years have witnessed an explosion of interest towards non-Hermitian quantum systems [12–15]. The ensuing physics often arises from considering open quantum systems interacting with their environment in the manner of Lindblad and continuous monitoring together with postselection [16,17], giving rise to many unexpected phenomena with no obvious counterpart in a Hermitian setting. One unique feature of non-Hermitian systems is the anomalous localization of all eigenstates referred to as the non-Hermitian skin effect [18–20] when all single-particle eigenstates become exponentially localized at the boundaries of the system. A paradigmatic model associated with this is the Hatano-Nelson [21,22] model, where the breakdown of reciprocity, i.e., asymmetric hoppings, induces the skin effect. While this occurs at the single-particle level, several studies addressed the fate of the non-Hermitian skin effect in a many-body setting, including numerics [23–29] as well as the Bethe ansatz [30,31].

Here, we go one step further and combine the above two concepts, namely full counting statistics and non-Hermitian physics, by analyzing the probability distribution of the particle number over a finite interval for the interacting Hatano-Nelson chain. By using bosonization, we solve the low-energy effective theory exactly and obtain analytical results for the real-space density profile, the correlation function of the oscillating part of the particle density, as well as the characteristic function of the particle density over a finite interval. We find that many-body physics suppresses significantly the non-Hermitian skin effect both for fermions and bosons. The Friedel oscillations exhibit a beating pattern as the Fermi wave number gets modified by the presence of an imaginary vector potential. In spite of the skin effect at the single-particle level, the probability distribution of particle density over a finite interval remains normal and depends on the location of the interval within the open chain. The mean value of the normal distribution scales with the imaginary vector potential while the variance becomes independent from

*dora.balazs@ttk.bme.hu

 

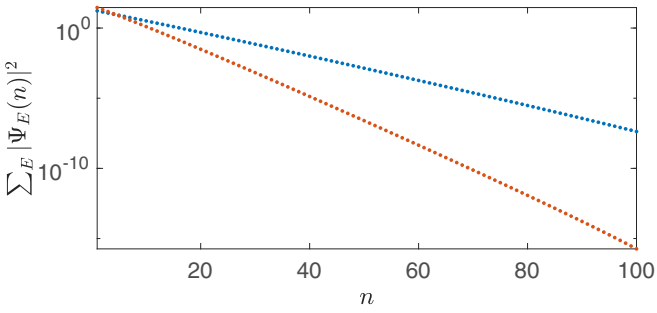


FIG. 1. Sum of absolute squares of amplitudes per site [12] of all right single-particle eigenstates of the noninteracting $H_{\rm HN}$ with $U = 0$, $N = 100$, and OBC with $ha = 0.1$ (upper blue) and 0.2 (lower red), exhibiting the non-Hermitian skin effect.

it. Our analytical findings are corroborated by several numerically exact methods even for relatively small systems.

## II. HATANO-NELSON MODEL

The Hatano-Nelson model [21,22] consists of fermions hopping in one dimension in the presence of an imaginary vector potential. The interacting many-body version of the Hamiltonian is

$$H_{\rm HN} = \sum_{n=1}^{N-1} \frac{J}{2} \exp(ah) c_n^+ c_{n+1} + \frac{J}{2} \exp(-ah) c_{n+1}^+ c_n + U c_n^+ c_n c_{n+1}^+ c_{n+1}, \tag{1}$$

where $J$ is the uniform hopping, $h$ is the constant imaginary vector potential and $a$ represents the lattice constant, $N$ is the total number of lattice sites and we consider the open boundary condition (OBC), and $U$ represents the the nearest-neighbor interaction between particles. We consider half filling with $N/2$ fermions populating the lattice. The model is $\mathcal{PT}$ symmetric [32] and possesses a real spectrum for OBC, and the minimal energy configuration is the ground state with a many-body wave function $|\Psi\rangle$. Due to OBC, no current is expected to flow in the system but the real-space density profile is expected to be inhomogeneous due to the imaginary vector potential. For a periodic boundary condition, a finite persistent current circulates in the system [33,34] but the real-space density profile is homogeneous.

In the noninteracting, $U = 0$ limit, the model can be diagonalized and the single-particle eigenfunctions $\Psi_E(n)$ for eigenenergy $E$ can be obtained. With OBC, these are localized to one end of the system (dictated by the sign of $h$) as a manifestation of the non-Hermitian skin effect. This is shown in Fig. 1.

Upon going to the continuum limit and bosonizing $H_{HN}$ in Eq. (1) [35–37], the effective low-energy Hamiltonian reads as

$$H = \int_0^L \frac{dx}{2\pi} v \left[ K[\pi \Pi(x) - i\pi h]^2 + \frac{1}{K} [\partial_x \phi(x)]^2 \right], \tag{2}$$

where $\Pi$ and $\phi$ are dual fields satisfying $[\phi(x_1), \Pi(x_2)] = i\delta(x_1 - x_2)$. This Hamiltonian is brought into conventional Hermitian Gaussian form by applying a similarity transformation, which eliminates the $ih$ term using $S^{-1}HS$ with

$$S = \exp\left( -\frac{h}{\pi} \int_0^L \phi(x') dx' \right). \tag{3}$$

The resulting Hamiltonian can be brought to diagonal form after introducing canonical bosonic fields [35] as

$$H_b = \sum_{q>0} \omega(q) b_q^\dagger b_q, \tag{4}$$

and the long-wavelength part of the local charge density is $\partial_x \phi(x)/\pi$ with

$$\phi(x) = i \sum_{q>0} \sqrt{\frac{\pi K}{qL}} \sin(qx) [b_q - b_q^\dagger] \tag{5}$$

for OBC and $K$ the Luttinger liquid (LL) parameter [35] [which carries all the nonperturbative effects of interaction $U$ from Eq. (1)], and $\omega(q) = vq$ with $v$ the Fermi velocity in the interacting systems, and $q = l\pi/L$ with $l = 1, 2, 3 \ldots$. The ground state of Eq. (4) is the vacuum state $|0\rangle$, and the ground state of the original non-Hermitian model is obtained as $|\Psi\rangle = S|0\rangle/\sqrt{\langle 0|S^2|0\rangle}$ and $S$ is Hermitian. The very fact that we managed to manipulate the low-energy effective theory into Eq. (4) indicates that the interacting Hatano-Nelson model indeed forms a Luttinger liquid with collective bosonic excitations in much the same way as for Hermitian systems [35].

Any expectation value of an operator $\mathcal{O}$ is evaluated as

$$\langle \Psi | \mathcal{O} | \Psi \rangle = \frac{\langle 0 | S \mathcal{O} S | 0 \rangle}{\langle 0 | S^2 | 0 \rangle}, \tag{6}$$

where the denominator accounts for the explicit normalization of the many-body wave function.

## III. CHARACTERISTIC FUNCTION OF PARTICLE DENSITY

We focus our attention on the characteristic function of particle density [38,39] in a finite spatial interval (or vertex operator [40]), given by

$$G_\lambda(x, y) = \langle \Psi | \exp\left[ 2i\lambda (\phi(x) - \phi(y)) \right] | \Psi \rangle, \tag{7}$$

where $\frac{1}{\pi}[\phi(x) - \phi(y)] = \sum_{n>y}^{x} c_n^+ c_n$ with $x > y$ is the particle number operator within the finite interval from $y$ to $x$ and the equality is valid within the realm of the low-energy theory [38]. Due to OBC, the system is not translationally invariant, therefore the characteristic function depends not only on $x - y$ but independently on the two coordinates.

From this, the long wavelength and $2k_F$ oscillating part of the density are obtained as

$$n_0(x) = \frac{1}{\pi} \lim_{\lambda \to 0} \partial_x G_\lambda(x, 0)/(2i\lambda), \tag{8a}$$

$$n_{2k_f}(x) = G_1(x, 0), \tag{8b}$$

and at half filling and $h = 0$, $k_F = \pi/2a$. By repeating this procedure, any higher moments of the density can be easily evaluated and by Fourier transforming with respect to $\lambda$, the distribution function of the density over a finite interval $x - y$ can be obtained for the interacting Hatano-Nelson model.

In evaluating Eq. (7), we use $[\phi(x), \phi(y)] = 0$, which allows us to merge all exponentials into a single one as

$$G_\lambda(x,y) = \frac{\langle 0|\exp\left(2i\lambda(\phi(x)-\phi(y)) - \frac{2h}{\pi}\int_0^L \phi(x')dx'\right)|0\rangle}{\langle 0|\exp\left(-\frac{2h}{\pi}\int_0^L \phi(x')dx'\right)|0\rangle}. \quad (9)$$

Then, profiting from the fact that the expectation value now is taken with respect to the bosonic vacuum, we use the standard trick to evaluate the expectation value of the exponentiated operator [35,40] to yield

$$\ln G_\lambda(x,y) = 2\langle 0|\left(i\lambda(\phi(x)-\phi(y)) - \frac{h}{\pi}\int_0^L \phi(x')dx'\right)^2|0\rangle - 2\langle 0|\left(\frac{h}{\pi}\int_0^L \phi(x')dx'\right)^2|0\rangle. \quad (10)$$

The term proportional to $h^2$ drops out and after taking the expectation values, and the characteristic function is evaluated as

$$\ln G_\lambda(x,y) = -2\lambda^2 C(x,y) - \frac{4i\lambda hL}{\pi}[g(x)-g(y)], \quad (11)$$

with

$$C(x,y) = \langle 0|[\phi(x)-\phi(y)]^2|0\rangle, \quad (12a)$$

$$g(x) = \int_0^L \frac{dx'}{L}\langle 0|\phi(x)\phi(x')|0\rangle. \quad (12b)$$

Here, the first term represent the autocorrelator of the $\phi$ field with open boundary conditions [36], while the second term carries all effects of the non-Hermitian term. These are evaluated to yield

$$\frac{1}{K}C(x,y) = \ln\left(\frac{L}{\pi\alpha}\right) + \frac{1}{2}\ln\left[\sin\left(\frac{\pi x}{L}\right)\sin\left(\frac{\pi y}{L}\right)\right] + \ln\left[\sin\left(\frac{\pi|x-y|}{2L}\right)\right] - \ln\left[\sin\left(\frac{\pi(x+y)}{2L}\right)\right], \quad (13)$$

$$g(x) = \frac{K}{\pi}\mathrm{Im}\sum_{\beta=\pm}\beta\,\mathrm{polylog}\left[2, \beta\exp\left(\frac{i\pi x}{L}\right)\right], \quad (14)$$

where $\alpha$ is the short distance cutoff in the theory, a remnant of the lattice constant in the $a \to 0$ continuum limit, and $\mathrm{polylog}(2,x)$ is the second-order polylogarithm [41]. This is valid in the scaling limit when $L \gg [x, y, x+y, |x-y| \mathrm{mod}\, L] \gg \alpha$. This immediately allows us to obtain the long-wavelength part of the density profile as

$$n_0(x) = -\frac{2Kh}{\pi^2}\ln\left[\tan\left(\frac{\pi x}{2L}\right)\right] \quad (15)$$

on top of the homogeneous particle background. We note that obtaining this result already in the noninteracting, $K = 1$ limit is far from being trivial due to the nonorthogonality of the single-particle eigenfunctions. For repulsive interactions ($K < 1$), the profile flattens out as the particles repel each other, while for the attractive case ($K > 1$), the inhomogeneous profile becomes more prominent as a remnant of the non-Hermitian skin effect. Interestingly, the very same low-energy effective theory applies not only to fermions but to repulsively interacting bosons as well, which then do not condense to one end of the sample but produce a smooth density profile due to repulsion.

## IV. FRIEDEL OSCILLATIONS

On top of the long-wavelength part, there is also a contribution oscillating [42,43] with $2k_F$. Putting everything together using Eqs. (8), the total particle density is

$$\rho(x) = \rho_0 + n_0(x) + c\left(\frac{\pi\alpha}{2L\sin\left(\frac{\pi x}{L}\right)}\right)^K \sin\left(2k_F x + \frac{4hL}{\pi}g(x) + \delta\right), \quad (16)$$

where $\rho_0$ represents the homogeneous background, and the coefficients $c$ and $\delta$ are in principle model as well as $K$ and $h$ dependent [36] and cannot be obtained from the low-energy theory. For $h = 0$, there are no Friedel oscillations at half filling since $2k_F x$ is an integer multiple of $\pi$ on the lattice due to $k_F = \pi/2a$, which makes the oscillations vanish for $\delta = 0$. Equation (16) represents one of our most important results which indicate that (i) the homogeneous density profile gets modified by the imaginary vector potential, (ii) the spatial decay of the oscillating term remains intact compared to the Hermitian case and (iii) the oscillation frequency picks up an anomalous term through $hLg(x)$.

Close to the middle of the chain, $g(L/2) = 2GK/\pi$ with $G \approx 0.916$ the Catalan's constant, and the oscillation frequency is also modulated by the imaginary vector potential. Close to the end of the chain, we obtain an effective $x$-dependent wave number, summarized as

$$k_F(x) = k_F + \frac{2}{\pi}hK \times \begin{cases} \frac{4}{\pi}G, & x \simeq L/2, \\ \ln\left(\frac{2eL}{x\pi}\right), & x \ll L/2. \end{cases} \quad (17)$$

We compare the prediction of Eqs. (16) and (17) to the numerics using exact diagonalization (ED) and density-matrix renormalization group (DMRG) [44] calculations of Eq. (1) at half filling, similarly to Ref. [45].

We employed the natural density matrix basis convention [46] in which the density matrix is constructed solely from the right eigenstate of the Hamiltonian when performing ED and DMRG. This allows us to compare the expectation values and the correlation functions of interest with the analytical findings derived using (6). This is the most suitable choice, and is the natural extension of the Hermitian realm, and such a description also follows naturally from an open quantum system perspective [16]. In the latter case, the Lindblad equation approach combined with continuous monitoring and postselection yields non-Hermitian physics, where expectation values are taken with respect to the right eigenstates.

For the Hermitian case with $h = 0$, the particle density is homogeneous and is fixed to $\rho_0 = 1/2$ even with OBC and interactions.

It is plausible to assume that we can still use the LL parameter [35], $K = \pi/2/[\pi - \arccos(U/J)]$, valid for $h = 0$, also for small $h$. It is remarkable that by using $c = 1/2$ and

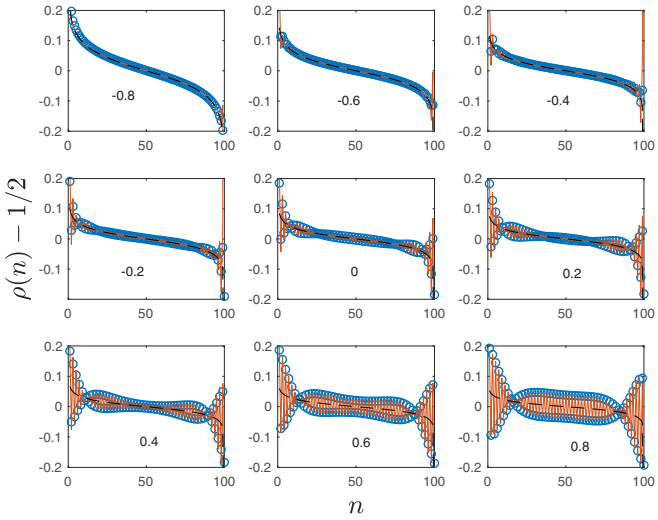


FIG. 2. Real-space density profile and Friedel oscillations for $U/J = -0.8 : 0.2 : 0.8$ as indicated in the panels, $N = 100$, and OBC with $ha = 0.1$. The open circles denote the numerical data from DMRG, while the red solid line represents bosonization from Eq. (16) with $c = 1/2$, $\delta = 0$, and $L = N\alpha$. The black dashed line depicts the long-wavelength contribution from Eq. (15).

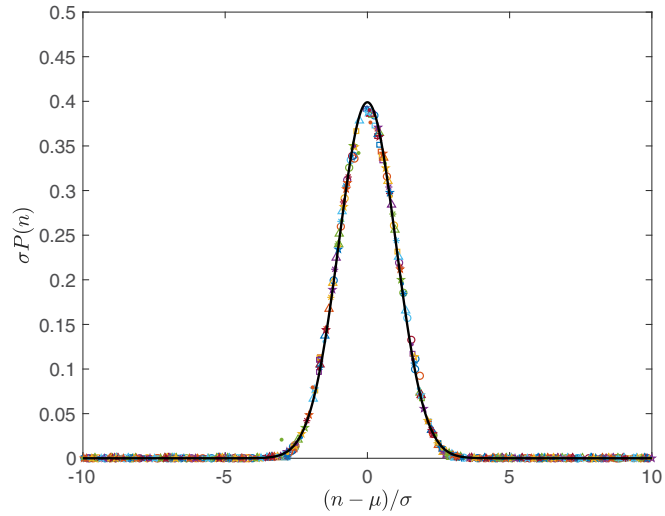


FIG. 3. Probability distribution of the density of particles in the first half of the chain ($N/2$ sites) from ED ($N \leqslant 28$) and DMRG ($N = 80$) for $U/J = -0.8 : 0.2 : 0.8$ and for $ah = 0.1$ and $N = 28$ (circle), 26 (square), for $ah = 0.2$ and $N = 28$ (triangle), 24 (star), and 80 (pentagram), and for $ah = 0.3$ and $N = 80$ (dot). The black solid line denotes the standard normal distribution.

$\delta = 0$ for all data in Fig. 2 as the only free parameters, we obtain very good agreement with numerics with $L = N\alpha$. The effect of the modulated Fermi wave number from Eq. (17) is visible in Fig. 2, especially close to the boundary. In spite of the strong localization of all single-particle eigenfunctions in the noninteracting case due to the non-Hermitian skin effect, the Friedel oscillations display rather smooth, nonlocalized behavior due the many-body effects.

## V. CORRELATION FUNCTION

The characteristic function in Eq. (7) allows us to evaluate equal time correlation functions as well. Most importantly, $G_1(x, y)$ represents the correlation function of the oscillating part of the particle density, which is responsible for the most dominant charge ordering instability [35,37] for repulsive interactions. Equations (12)–(14) together with (17) predict the behavior of this correlation function. The spatial decay is dictated by $C(x, y)$ and receives the very same exponent $K$ as for the Hermitian system [35,36]. The non-Hermitian term, however, modulates its oscillation frequency from $2k_F$ through $\exp[2ik_F(x)x - 2ik_F(y)y]$.

## VI. PROBABILITY DISTRIBUTION OF THE DENSITY

By the $\lambda$ dependence of the characteristic function, it is apparent that it corresponds to the normal distribution with mean ($\mu$) and variance ($\sigma^2$) given by

$$\mu = \frac{2hL}{\pi^2}[g(x) - g(y)], \quad \sigma^2 = \frac{1}{\pi^2}C(x, y). \tag{18}$$

From Eqs. (13) and (14), both the mean and variance scales with $K$ and are enhanced/suppressed for attractive/repulsive interactions. Moreover, the mean scales linearly with the imaginary vector potential while the variance is insensitive to it within the validity of bosonization. We emphasize that the variance remains symmetric under the $(x, y) \longleftrightarrow (L - x, L - y)$ transformation, namely the fluctuations are insensitive to which end of the system we consider, while the skin effect in Fig. 1 clearly distinguishes the two ends of the chain within the realm of single-particle physics.

In the following, we analyze their behavior for some relevant spatial range. Close to the middle of the chain with $x, y \simeq L/2$, boundary effects are the most negligible as depicted in Table I, where the variance depends only on $x - y$ and agrees with Ref. [38], while the mean value is negligibly small. On the other hand, close to the boundary of the system, the dependence on $x$ and $y$ independently from each other becomes more prominent as summarized in Table I. Finally, we also consider the case with $y = 0$ and $x = L/2$ in Table I, i.e., the distribution of particles in the first half of the chain.

In order to test the Gaussian nature of the particle distribution, we analyze the distribution of particles in the first half of the chain, namely $N_1 = \sum_{n=1}^{N/2} c_n^+ c_n$, which can take integer values from 0 to $N/2$. Using ED and DMRG, we evaluated numerically the characteristic function of the particle density, $\langle\Psi|\exp(i\lambda N_1)|\Psi\rangle$ and after Fourier transforming with respect to $\lambda$, the probability distribution of the particle density is obtained. We plot this for several interaction strengths, ranging

TABLE I. Parameters of the normal distribution for various spatial intervals.

| Region | $\mu/hK$ | $\sigma^2\pi^2/K$ |
|---|---|---|
| $x, y \simeq \frac{L}{2}$ | $\frac{1}{\pi L}(x - y)(L - x - y)$ | $\ln\left(\frac{\lvert x-y\rvert}{2\alpha}\right)$ |
| $x, y \ll L$ | $\frac{2}{\pi^2}[x\ln(\frac{2eL}{x\pi}) - y\ln(\frac{2eL}{y\pi})]$ | $\ln\left(\frac{\sqrt{xy}\lvert x-y\rvert}{\alpha(x+y)}\right)$ |
| $(x, y) = (\frac{L}{2}, 0)$ | $\frac{4GL}{\pi^3}$ | $\frac{1}{2}\ln\left(\frac{L}{\pi\alpha}\right)$ |

from strongly attractive through noninteracting to strongly repulsive and for several $h$ in Fig. 3, after rescaling it with the mean and the variance. All data fall onto a universal curve, dictated by the standard normal distribution $P(n) = \exp(-n^2/2)/\sqrt{2\pi}$. Already for relatively small system sizes, the data collapse is excellent, confirming the prediction and validity of bosonization not only for simple expectation values but also for the full distribution function in non-Hermitian systems.

## VII. CONCLUSIONS

We have studied the full counting statistics of particle density in the interacting Hatano-Nelson model. While the non-Hermitian skin effects localize the single-particle states to one end of the chain, the many-body density profile becomes smooth along the chain, indicating the suppression of the skin effect by many-body physics. Friedel oscillations appear throughout the system with a beating pattern, which arises from a spatially dependent Fermi wave vector due to the imaginary vector potential.

The correlation function of the oscillating part of the particle density, which accounts for the dominant instability for repulsive interactions, decays similarly to the Hermitian case albeit its spatial modulation is influenced by the non-Hermitian term. The probability distribution of particles over any finite interval is found to be normal with the mean scaling with the imaginary vector potential in spite of the non-Hermitian skin effect, which suppresses exponentially the single-particle eigenfunctions in one end of the chain.

Our results apply not only to interacting fermions in the Hatano-Nelson model, but the very same low-energy effective theory through Eqs. (4) and (5) accounts for repulsively interacting bosons [35] as well. Our findings indicate that some peculiar features of single-particle non-Hermitian physics can be washed out in the many-body realm and non-Hermitian many-body systems behave rather similarly to their Hermitian counterparts not only at the level of simple expectation values but also for the full counting statistics.

## ACKNOWLEDGMENTS

This research is supported by the National Research, Development and Innovation Office - NKFIH within the Quantum Technology National Excellence Program (Project No. 2017-1.2.1-NKP-2017-00001), K134437, and K142179, by the BME-Nanotechnology FIKP grant (BME FIKP-NAT), and by a grant of the Ministry of Research, Innovation and Digitization, CNCS/CCCDI-UEFISCDI, under Project No. PN-III-P4-ID-PCE-2020-0277.

[1] H. Fischer, *A History of the Central Limit Theorem* (Springer, New York, 2021).
[2] H. Touchette, The large deviation approach to statistical mechanics, Phys. Rep. **478**, 1 (2009).
[3] E. Bertin, Global Fluctuations and Gumbel Statistics, Phys. Rev. Lett. **95**, 170601 (2005).
[4] D. P. Arovas, E. Berg, S. A. Kivelson, and S. Raghu, The Hubbard model, Annu. Rev. Condens. Matter Phys. **13**, 239 (2022).
[5] M. Campisi, P. Hänggi, and P. Talkner, Colloquium: Quantum fluctuation relations: Foundations and applications, Rev. Mod. Phys. **83**, 771 (2011).
[6] Y. Ashida and M. Ueda, Full-Counting Many-Particle Dynamics: Nonlocal and Chiral Propagation of Correlations, Phys. Rev. Lett. **120**, 185301 (2018).
[7] L. S. Levitov, H. Lee, and G. B. Lesovik, Electron counting statistics and coherent states of electric current, J. Math. Phys. **37**, 4845 (1996).
[8] I. L. S. Hofferberth, T. Schumm, A. Imambekov, V. Gritsev, E. Demler, and J. Schmiedmayer, Probing quantum and thermal noise in an interacting many-body system, Nat. Phys. **4**, 489 (2008).
[9] V. Gritsev, E. Altman, E. Demler, and A. Polkovnikov, Full quantum distribution of contrast in interference experiments between interacting one-dimensional Bose liquids, Nat. Phys. **2**, 705 (2006).
[10] M. Gring, M. Kuhnert, T. Langen, T. Kitagawa, B. Rauer, M. Schreitl, I. Mazets, D. A. Smith, E. Demler, and J. Schmiedmayer, Relaxation and prethermalization in an isolated quantum system, Science **337**, 1318 (2012).
[11] G. Hercé, J.-P. Bureik, A. Ténart, A. Aspect, A. Dareau, and D. Clément, Full counting statistics of interacting lattice gases after an expansion: Quantifying many-body coherence from atom correlations, arXiv:2207.14070.
[12] E. J. Bergholtz, J. C. Budich, and F. K. Kunst, Exceptional topology of non-Hermitian systems, Rev. Mod. Phys. **93**, 015005 (2021).
[13] Y. Ashida, Z. Gong, and M. Ueda, Non-Hermitian physics, Adv. Phys. **69**, 249 (2020).
[14] I. Rotter and J. P. Bird, A review of progress in the physics of open quantum systems: Theory and experiment, Rep. Prog. Phys. **78**, 114001 (2015).
[15] R. El-Ganainy, K. G. Makris, M. Khajavikhan, Z. H. Musslimani, S. Rotter, and D. N. Christodoulides, Non-Hermitian physics and PT symmetry, Nat. Phys. **14**, 11 (2018).
[16] A. J. Daley, Quantum trajectories and open many-body quantum systems, Adv. Phys. **63**, 77 (2014).
[17] H. Carmichael, *An Open Systems Approach to Quantum Optics* (Springer, Berlin, 1993).
[18] T. E. Lee, Anomalous Edge State in a Non-Hermitian Lattice, Phys. Rev. Lett. **116**, 133903 (2016).
[19] S. Yao and Z. Wang, Edge States and Topological Invariants of Non-Hermitian Systems, Phys. Rev. Lett. **121**, 086803 (2018).
[20] F. K. Kunst, E. Edvardsson, J. C. Budich, and E. J. Bergholtz, Biorthogonal Bulk-Boundary Correspondence in Non-Hermitian Systems, Phys. Rev. Lett. **121**, 026808 (2018).
[21] N. Hatano and D. R. Nelson, Vortex pinning and non-Hermitian quantum mechanics, Phys. Rev. B **56**, 8651 (1997).

[22] N. Hatano and D. R. Nelson, Localization Transitions in Non-Hermitian Quantum Mechanics, Phys. Rev. Lett. **77**, 570 (1996).

[23] S.-B. Zhang, M. M. Denner, T. Bzdušek, M. A. Sentef, and T. Neupert, Symmetry breaking and spectral structure of the interacting Hatano-Nelson model, Phys. Rev. B **106**, L121102 (2022).

[24] F. Alsallom, L. Herviou, O. V. Yazyev, and M. Brzezińska, Fate of the non-Hermitian skin effect in many-body fermionic systems, Phys. Rev. Res. **4**, 033122 (2022).

[25] E. Lee, H. Lee, and B.-J. Yang, Many-body approach to non-Hermitian physics in fermionic systems, Phys. Rev. B **101**, 121109(R) (2020).

[26] R. Hamazaki, K. Kawabata, and M. Ueda, Non-Hermitian Many-Body Localization, Phys. Rev. Lett. **123**, 090603 (2019).

[27] S. Mu, C. H. Lee, L. Li, and J. Gong, Emergent Fermi surface in a many-body non-Hermitian fermionic chain, Phys. Rev. B **102**, 081115(R) (2020).

[28] D.-W. Zhang, Y.-L. Chen, G.-Q. Zhang, L.-J. Lang, Z. Li, and S.-L. Zhu, Skin superfluid, topological Mott insulators, and asymmetric dynamics in an interacting non-Hermitian Aubry-André-Harper model, Phys. Rev. B **101**, 235150 (2020).

[29] Z. Wang, L.-J. Lang, and L. He, Emergent Mott insulators and non-Hermitian conservation laws in an interacting bosonic chain with noninteger filling and nonreciprocal hopping, Phys. Rev. B **105**, 054315 (2022).

[30] T. Fukui and N. Kawakami, Breakdown of the Mott insulator: Exact solution of an asymmetric Hubbard model, Phys. Rev. B **58**, 16051 (1998).

[31] L. Mao, Y. Hao, and L. Pan, Non-Hermitian skin effect in one-dimensional interacting Bose gas, arXiv:2207.12637.

[32] C. M. Bender, Making sense of non-Hermitian Hamiltonians, Rep. Prog. Phys. **70**, 947 (2007).

[33] I. Affleck, W. Hofstetter, D. R. Nelson, and U. Schollwöck, Non-Hermitian Luttinger liquids and flux line pinning in planar superconductors, J. Stat. Mech.: Theory Exp. (2004) P10003.

[34] W. Hofstetter, I. Affleck, D. Nelson, and U. Schollwöck, Non-Hermitian Luttinger liquids and vortex physics, Europhys. Lett. **66**, 178 (2004).

[35] T. Giamarchi, *Quantum Physics in One Dimension* (Oxford University Press, Oxford, UK, 2004).

[36] M. A. Cazalilla, Bosonizing one-dimensional cold atomic gases, J. Phys. B: At., Mol. Opt. Phys. **37**, S1 (2004).

[37] A. O. Gogolin, A. A. Nersesyan, and A. M. Tsvelik, *Bosonization and Strongly Correlated Systems* (Cambridge University Press, Cambridge, UK, 1998).

[38] H. F. Song, S. Rachel, and K. Le Hur, General relation between entanglement and fluctuations in one dimension, Phys. Rev. B **82**, 012405 (2010).

[39] M. Arzamasovs and D. M. Gangardt, Full Counting Statistics and Large Deviations in a Thermal 1D Bose Gas, Phys. Rev. Lett. **122**, 120401 (2019).

[40] J. von Delft and H. Schoeller, Bosonization for beginners–refermionization for experts, Ann. Phys. **510**, 225 (1998).

[41] I. Gradshteyn and I. Ryzhik, *Table of Integrals, Series, and Products* (Academic Press, New York, 2007).

[42] J. Friedel, XIV. The distribution of electrons round impurities in monovalent metals, Philos. Mag. **43**, 153 (1952).

[43] B. Skinner, Friedel oscillations: Wherein we learn that the electron has a size (2009), Gravity and Levity blog, https://gravityandlevity.wordpress.com.

[44] S. R. White, Density Matrix Formulation for Quantum Renormalization Groups, Phys. Rev. Lett. **69**, 2863 (1992).

[45] B. Dóra and C. P. Moca, Quantum Quench in $\mathcal{PT}$-Symmetric Luttinger Liquid, Phys. Rev. Lett. **124**, 136802 (2020).

[46] L. Herviou, N. Regnault, and J. H. Bardarson, Entanglement spectrum and symmetries in non-Hermitian fermionic non-interacting models, SciPost Phys. **7**, 069 (2019).